自适应斜Z字形采样Hadamard单像素成像

苏杰[1]，翟爱平[2]，赵文静[2]，韩青[1]，王东[1,2]
（1 太原理工大学 新型传感器与智能控制教育部重点实验室,太原030024）
（2 太原理工大学 物理与光电工程学院,太原030024）

摘　要：单像素成像技术在成像速度和质量上已经取得一定的进展,然而,如何在保证成像质量的前提下提升成像速度仍然是一个待解决的问题。对Hadamard系数矩阵中每条斜列上的系数绝对值求取平均值后,发现其具有迅速减小的特征,基于此发现提出了一种自适应斜Z字形采样方法,以实现预期的成像质量和速度提升。实验结果表明,该方法可以有效减少采样次数与数据采集量,兼顾成像质量的同时提升了成像速度。在相同的采样率下,其成像质量优于顺序采样的单像素成像。

关键词：单像素成像;Hadamard变换;Hadamard系数;自适应;Z字形采样

中图分类号：TP399　　　　**文献标识码**：A　　　　　**doi**：10.3788/gzxb20215003.0311003

Hadamard Single-pixel Imaging Using Adaptive Oblique Zigzag Sampling

SU Jie[1], ZHAI Aiping[2], ZHAO Wenjing[2], HAN Qing[1], WANG Dong[1,2]
（1 *Key Laboratory of Advanced Transducers and Intelligent Control Systems*，*Ministry of Education and Shanxi Province*，*Taiyuan University of Technology*，*Taiyuan* 030024，*China*）
（2 *College of Physics and Optoelectronics*，*Taiyuan University of Technology*，*Taiyuan* 030024，*China*）

Abstract：Single-pixel imaging has made significant progress in imaging quality and speed. However，how to improve the imaging speed while ensuring the imaging quality is still a problem to be solved. Based on the finding that the average value of the absolute value of the Hadamard coefficients of each oblique line declines rapidly，an adaptive oblique zigzag sampling method is proposed to achieve the expected imaging speed and quality. Experimental results show that the number of sampling and the amount of data acquisition can be effectively reduced using the proposed method，improving the imaging speed while ensuring the imaging quality. Compared with the single-pixel imaging using sequential sampling，the imaging quality of the proposed method is better under the same sampling rate.

Key words：Single-pixel imaging；Hadamard transform；Hadamard coefficients；Adaptive；Zigzag sampling

OCIS Codes：110.1085；110.1758；100.3010

http：// *www* .*photon* .*ac* .*cn*

0 Introduction

Single-pixel Imaging (SPI), which is different from traditional imaging, has its advantages. For example, in infrared and terahertz imaging, traditional array-based imaging sensors and systems are relatively bulky, complicated, and usually demand additional auxiliary modules which make them expensive. In contrast, SPI provides a better solution in which only a single point detector is needed, and the setup of the system is simple, which significantly reduces the costs. It is developed with the advent of the Compressed Sensing (CS) theory. In 2006, DONOHO D L [1] and CANDÈS E J [2] proposed the CS theory. In 2008, DUARTE M F [3] realized the SPI based on CS, which suggested that CS [1-6] had a broad prospect in the field of SPI. In addition to CS, Hadamard Transform (HT) [7-15], Fast Fourier Transform (FFT) [14-21], Wavelet transform [15, 22] and so on have been used in SPI to reconstruct the object, due to the low hardware requirements, short imaging time, and good imaging performance. Among them, HT has the merits of deterministic orthogonal basis patterns and can produce binary patterns that can be conveniently implemented by a Spatial Light Modulator (SLM) such as a digital Micro-Mirror Device (DMD). Therefore, it is widely utilized in SPI.

However, with the increase of the imaging resolution, the measurements of SPI increase greatly, thus the imaging speed is limited. To solve this problem, current solutions are mainly to improve the sampling speed of the equipment or optimize the algorithm. At present, the generation of spatially structured light mainly depends on the SLM, but as its performance increases, its costs will increase. Therefore, XU Zihao et al.[23] proposed a computational ghost imaging scheme using LED-based high-speed lighting modules, which is a low-cost SPI scheme. However, it is only suitable for short-distance and low-resolution imaging, and its imaging resolution is limited. Reducing samplings through algorithm optimization is a cost-effective way to improve the imaging speed of SPI. The potential solution is to use the sparsity or compressibility of the signal to make a smaller number of measurements i.e. reducing the sampling rate of the SPI.

Here, based on the collected Hadamard spectrum, it is found that the distribution of the Hadamard spectrum has sparse characteristics, and the average value of the absolute value of the Hadamard coefficients in the oblique line shows a decreasing trend from the upper left to the lower right of the Hadamard spectrum. When it drops to a certain value, its implication on SPI is relatively weak. Taking this fact into consideration, an adaptive oblique zigzag sampling method is proposed and demonstrated to achieve a balance between the expected imaging fidelity and speed. It averages each oblique line of the absolute value of Hadamard coefficients along the oblique zigzag direction from the upper left corner to the lower right corner of the spectrum and compares the results with a threshold set by the user to automatically discard high-frequency signals and noises according to the expected imaging fidelity. Because only when the average values are larger than the set threshold, the Hadamard coefficients are collected, the sampling rate will be adaptively reduced to achieve a balance between imaging speed and the expected imaging fidelity.

1 Principle

1.1 SPI based on HT

Assuming that a digital image is represented as $O(x, y)$ and its resolution is $M \times N$, then its sparse representation in Hadamard domain can be expressed as

$$I_{\mathrm{H}}(u, v) = H\{O(x, y)\} = \frac{1}{MN} \sum_{x=0}^{M-1} \sum_{y=0}^{N-1} O(x, y)(-1)^{\sum_{i=0}^{N-1}[b_i(x)b_i(u) + b_i(y)b_i(v)]} \tag{1}$$

inverse Hadamard transformation of the Hadamard coefficients matrix $I_{\mathrm{H}}(u, v)$ can be expressed as

$$O(x, y) = \sum_{x=0}^{M-1} \sum_{y=0}^{N-1} H\{O(x, y)\}(-1)^{\sum_{i=0}^{N-1}[b_i(x)b_i(u) + b_i(y)b_i(v)]} \tag{2}$$

where (u, v) are the coordinates in Hadamard domain. $H\{\}$ is the HT calculation. (x, y) are the coordinates in spatial domain. $b_k(z)$ is the kth bit of the binary representation of z.

Based on the above-mentioned HT, the orthogonal Hadamard basis patterns can be generated using the inverse HT calculation, which can be set and expressed as

$$\Theta(u, v) = \begin{cases} 1 & u = u_0, v = v_0 \\ 0 & \text{otherwise} \end{cases} \tag{3}$$

The generated Hadamard basis patterns are normalized, and can be expressed as

$$\phi_H(x, y) = \frac{1}{2} [1 + H^{-1}\{\Theta(u, v)\}] \tag{4}$$

where $H^{-1}\{\ \}$ is the inverse HT calculation, $u \in (0, 1, 2, 3, \cdots, M-1), v \in (0, 1, 2, 3, \cdots, N-1)$, and each pattern corresponds to a unique 'Hadamard-frequency' component.

To further improve the imaging fidelity, we adopt a differential algorithm[9] to suppress noise and improve the system of signal-to-noise. The basis pattern $\phi_H(x, y)$ generated by Eq.(4) is projected onto the object, and the reflected light signal $D_{+1}(u, v)$ is detected. Then, reversing the basic pattern $1 - \phi_H(x, y)$, the reflected light signal $D_{-1}(u, v)$ is detected. The absolute value of Hadamard coefficients matrix $S(u, v)$ can be obtained by

$$S(u, v) = D_{+1}(u, v) - D_{-1}(u, v) \tag{5}$$

therefore, the object can be reconstructed by calculating the inverse HT of it.

1.2　Adaptive oblique zigzag sampling

The proposed method makes full use of the fact that the low frequencies of Hadamard single-pixel imaging are concentrated on the upper left corner as shown in Fig. 1(b) and (c). Fig. 1(a) is the target image to be restored. Fig. 1(b) is the sequential sampling. After carefully investigating the Hadamard spectrum in Fig. 1(c), we found that the average value of the absolute value of the Hadamard coefficients for each oblique line has the characteristic that it decreases rapidly as shown in Fig. 1(d), which inspired us to propose the adaptive oblique zigzag sampling method to achieve a balance between the imaging fidelity and speed.
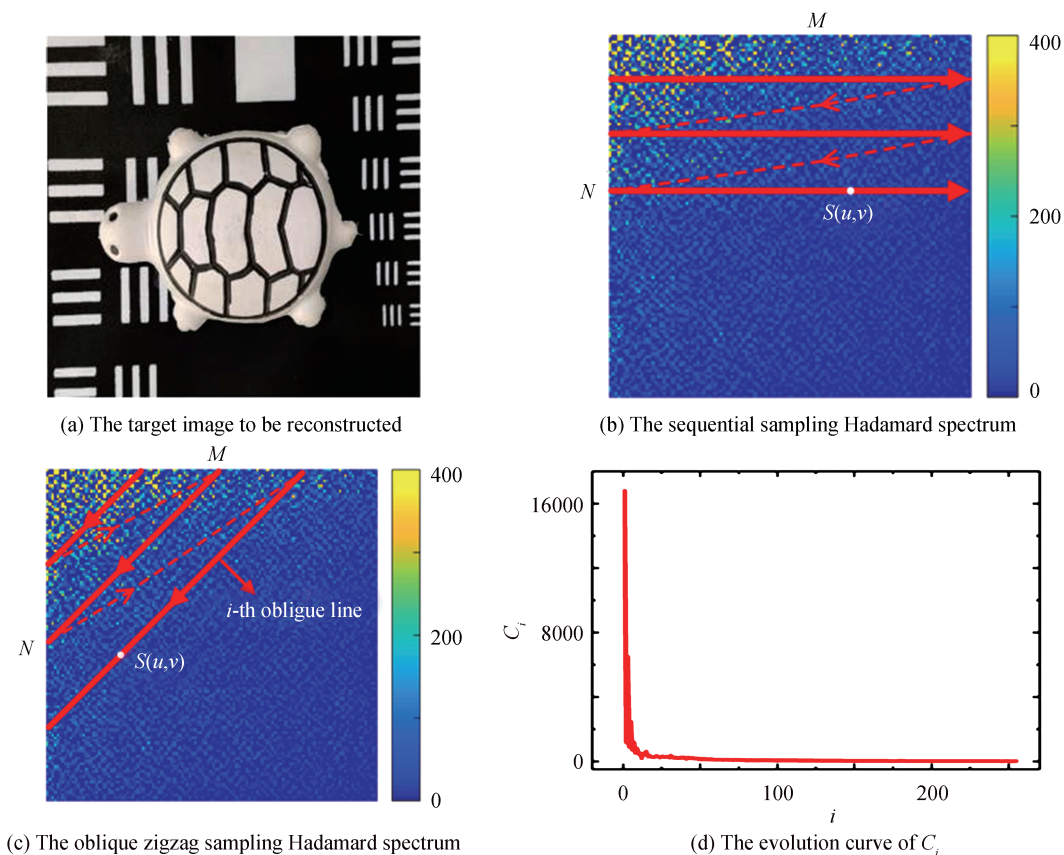

(a) The target image to be reconstructed

(b) The sequential sampling Hadamard spectrum

(c) The oblique zigzag sampling Hadamard spectrum

(d) The evolution curve of C_i

Fig.1　Two sampling paths of the target image and the evolution curve of C_i which is the average value of the absolute value of the Hadamard coefficients for each oblique line i

Most information on a natural object normally concentrates on the low-frequency components, and the subtle details and noise concentrate on the high-frequency components[14]. Therefore, effectively collecting the low-frequency components in the upper left corner and ignoring a few high-frequency components can reduce the sampling rate, and improve the imaging speed of the single-pixel camera.

As shown in Fig. 1(c), the low-frequency components are concentrated on the upper left corner of the Hadamard spectrum. We found that in the oblique zigzag direction from the upper left to the lower right of the spectrum, the average value of the absolute value of the Hadamard coefficients for each oblique line i can be calculated as

$$C_i = \frac{\sum\limits_{u+v=i-1} |\boldsymbol{S}(u, v)|}{i} \qquad (6)$$

in which the oblique line $i = 1, 2, 3, ..., \overbrace{N, ..., N}^{M-N+1}, ..., 3, 2, 1$, $M \geqslant N$, $|\boldsymbol{S}(u, v)|$ is the absolute value of the Hadamard coefficients. The evolution curve C_i is plotted in Fig. 1(d), which shows that the C_i rapidly decreases with the increase of the oblique line i. Therefore, sampling is performed in an oblique zigzag direction from the upper left corner to the lower right corner of the spectrum. A threshold C can be set to perform the adaptively sampling according to the desired imaging fidelity. Only when the average values are larger than the set threshold, the Hadamard coefficients are collected, the sampling rate will be adaptively reduced to achieve a balance between imaging speed and the expected imaging fidelity.

2 Experimental setup

As shown in Fig. 2, light emitted from an ultra-high-pressure mercury lamp incidents on the DMD coded by the basis of Hadamard patterns, which projects the coded illuminations onto the object. The light reflected from the illuminated object is detected by a photodetector (PD KG-PR-200K-A-FS), which converts the optical signal into an electrical signal. The electrical signal is collected by a digital acquisition card (NI USB-6216) to convert it to be a digital signal for computer processing. Finally, the image of the object can be reconstructed computationally.
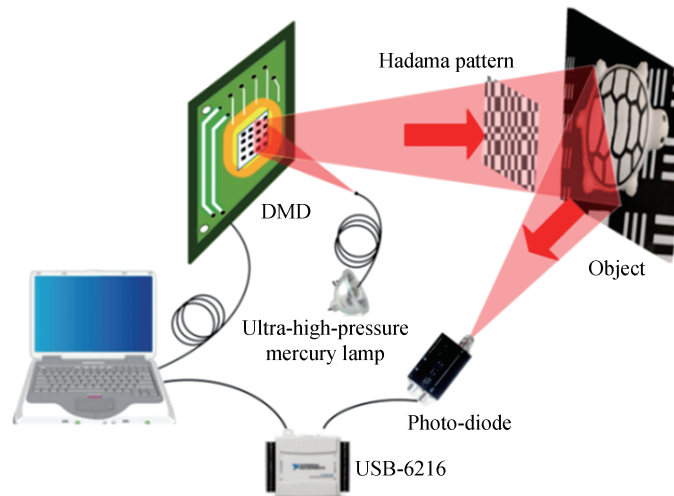

Fig. 2　Schematic diagram of the experimental setup

3 Results and discussion

We adopt the differential algorithm to improve the performance of Hadamard SPI and enhance the anti-interference ability to the system noise. Fig. 3(a) shows the object to be reconstructed. Fig. 3(b) is the image reconstructed without the differential algorithm. Due to the influence of the noise, the edge of the image is blurry. Fig. 3(c) is the reconstructed image after noise reduction by the difference algorithm, thus the contrast of it is better as compared to the reconstruction shown in Fig. 3(b). Besides, the reconstructed image has a

better fidelity，which shows that the differential algorithm has a strong anti-interference ability. In the experiments，we adopted the differential algorithm.
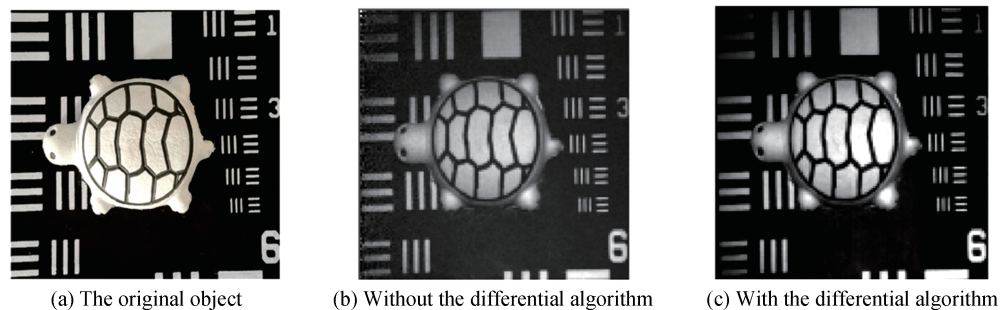

(a) The original object　　　(b) Without the differential algorithm　　　(c) With the differential algorithm

Fig.3　The reconstructed image of the object with a resolution of 128×128 pixels

To verify the effectiveness of the proposed oblique zigzag adaptive sampling method，the same object as shown in Fig. 3(a) was reconstructed by using the method in which the threshold C was set to be 0，200，300，and 400. The corresponding experimental results are given in Fig. 4，in which the horizontal coordinate i is the oblique line，and the vertical coordinate C_i calculated by Eq.(6)，is the average value of the absolute value of the Hadamard coefficients for each oblique line. Besides，there are two inserts，the left one is a zoom-in of the part indicated by the dashed ellipse and the right one is the reconstructed image of the object with a resolution of 128×128 pixels. As can be seen in Fig.4，the evolution curves decrease with the increase of the oblique line i，and there is a sharp decrease within $i < 20$ which suggests that the low-frequency components are concentrated within a small area（$i < 20$）at the upper left corner of the Hadamard spectrum matrix as predicted and shown in Fig. 1(c). It can be seen from the comparison of the evolution curves shown in Fig. 4(a)～(d) that，for the chosen threshold C_i equals to 0，200，300 and 400，the sampling rates are respectively 100％，46.17％，36.92％ and 22.04％，and the object can be successfully reconstructed，which suggests that，by setting different thresholds according to the expected imaging fidelity，the proposed method can adaptively sample along the

(a) $C=0$　　　　　　　　　　　　　　　　　　　(b) $C=200$
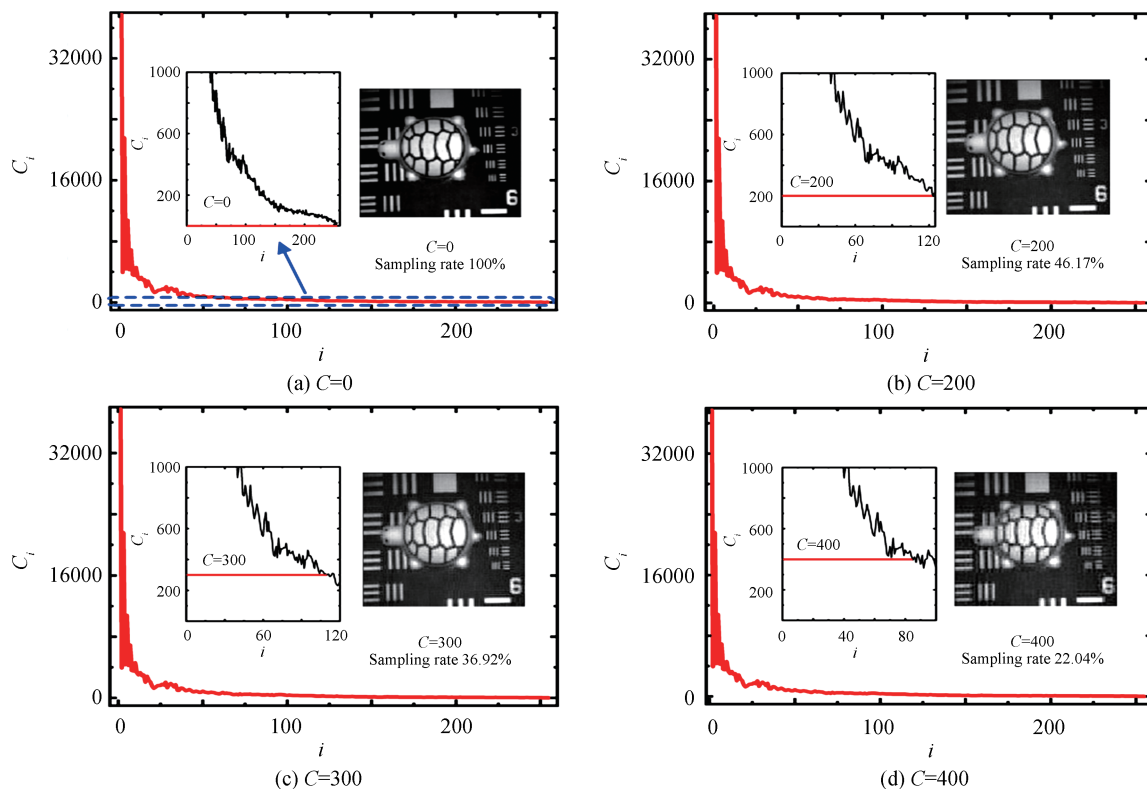
(c) $C=300$　　　　　　　　　　　　　　　　　　(d) $C=400$

Fig. 4　Reconstructed results of the object as well as the corresponding evolution curves

oblique zigzag path in Hadamard spectrum domain. Therefore, without the need for CS algorithms, it can efficiently collect the low-frequency components in the upper left corner and ignore a few high-frequency components to adaptively reduce the sampling rate for improving the imaging speed of the single-pixel camera.

Fig. 5 gives the results reconstructed using the proposed method and the sequential sampling method with the same sampling rates which are respectively 100%, 46.17%, 36.92%, and 22.04%. SSIM and PSNR [14] are used for assessing the reconstructed results in Fig. 5. The corresponding results are presented in Fig. 6(a) and (b). The red triangle and blue square lines respectively correspond to the proposed method and the sequential sampling method. As can be observed in Fig. 5, as the threshold C increases from 0, 200, 300 to 400, both PSNR and SSIM parameters show a downward trend. As predicted in Fig. 5(a), when the threshold C is 0, the corresponding sampling rate is 100%, and the quality of the reconstructed images is the best. The PSNR is close to positive infinity, and the SSIM is close to 1. As the threshold increases, PSNR and SSIM show a decreasing tendency. Under the same threshold, the red triangle line is always higher than the blue square line. Therefore, under the same sampling rate or threshold, the adaptive oblique zigzag sampling method is better than the sequential sampling method. Besides, the red triangle line decreases more slowly than the blue square line. As the threshold increases, the gap between the PSNR and SSIM parameters of the two sampling methods gradually increases. Therefore, by increasing the threshold (i.e. reducing the sampling rate), the image quality reconstructed by the adaptive zigzag sampling method is better.
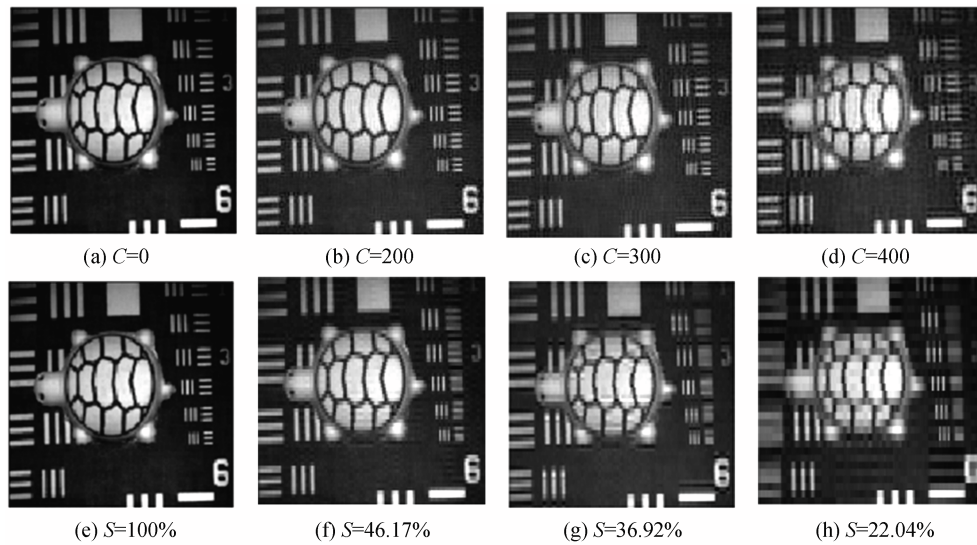

(a) C=0　　　　　(b) C=200　　　　　(c) C=300　　　　　(d) C=400

(e) S=100%　　　　(f) S=46.17%　　　　(g) S=36.92%　　　　(h) S=22.04%

Fig.5　Reconstructed objects using the adaptive oblique zigzag sampling method with a threshold $C=0$, threshold $C=200$, threshold $C=300$, threshold $C=400$; Reconstructed objects using the sequential sampling method setting the sampling rate as $S=100\%$, $S=46.17\%$, $S=36.92\%$, and $S=22.04\%$
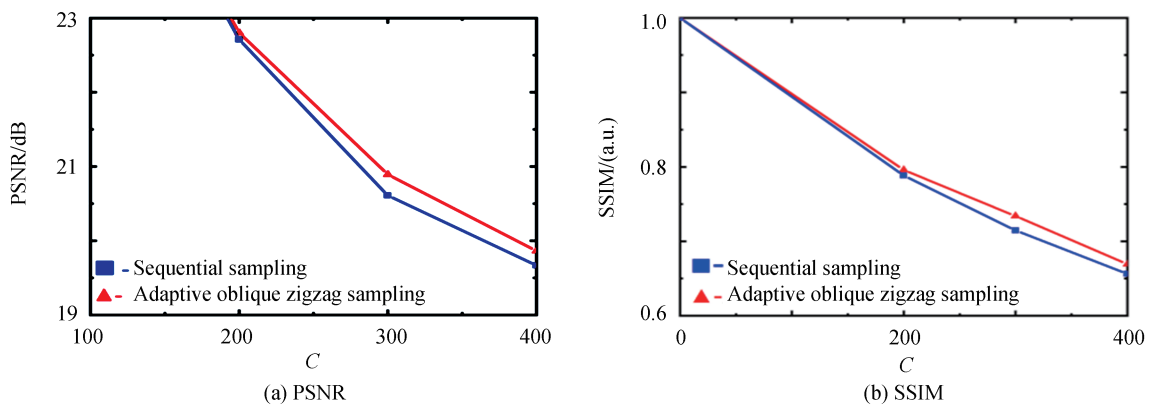

(a) PSNR　　　　　　　　　　　　　　(b) SSIM

Fig.6　PSNR and SSIM of the reconstructions using the two types of sampling strategies

To further investigate the influence of the dark noise of the PD on SPI using the proposed method. We measured the dark noise signals of two different PDs as shown in Fig. 7(a). The tortoise image with the resolution of 128×128 is reconstructed using the two PDs. The results are shown in Fig. 7(b). The smaller the dark noise of the PD, the better the quality of the reconstructed image, which suggests that the much of dark noise of the detection system can not be suppressed using the differential algorithm [14]. In this situation, during the experiments, it can be predicted from Fig. 7 that as the dark noise of the detector increases, the imaging quality will gradually deteriorate. When a PD with high dark noise, such as PD1, is used, the high frequencies of the object to be reconstructed will be drowned in the high-frequency noise, which means SPI using the fully sequential or zigzag sampling will not give a satisfactory result, this can be seen in Fig. 8(a) in which more samplings give poorer results due to the high-frequency dark noise. In this case, SPI using the proposed adaptive zigzag sampling is necessary and can automatically get rid of the high-frequency noise by setting an appropriate threshold C to get better reconstructions as shown in Fig. 8(b) and (c), at the same time a balance between imaging quality and speed can be achieved. As shown in Fig. 8, the three restored pictures are marked with a red dashed frame in the same place. As the threshold increases, the dark noise gradually decreases.
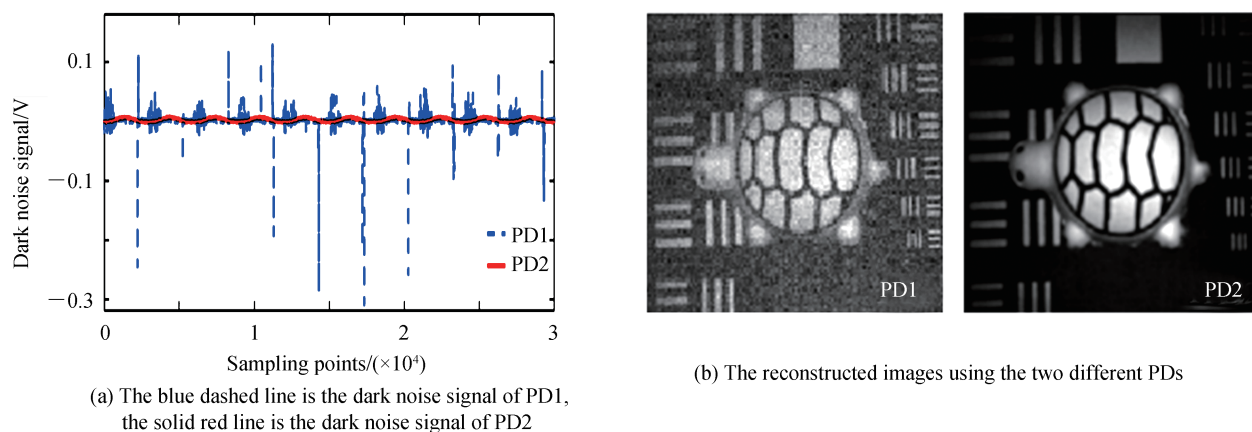

(a) The blue dashed line is the dark noise signal of PD1, the solid red line is the dark noise signal of PD2

(b) The reconstructed images using the two different PDs

Fig.7　The influence of PD dark noise signal on imaging results

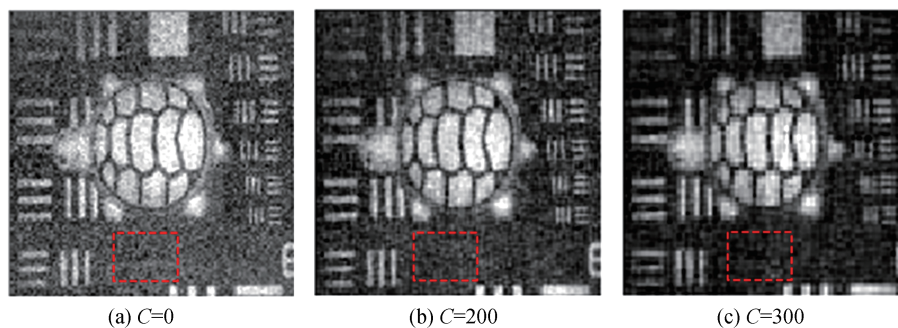(a) $C=0$　　　　　　(b) $C=200$　　　　　　(c) $C=300$

Fig.8　SPI using PD1 and the adaptive oblique zigzag sampling with the thresholds

A Hadamard SPI using the proposed adaptive oblique zigzag sampling method has been proposed and demonstrated. Hadamard transform is one of the orthogonal transforms, therefore, the proposed method not only can apply to other orthogonal transform based SPIs, but also inherits the advantages of orthogonal transform based SPIs.

As indicated in Ref.[21], compared with the traditional compressed sensing method, orthogonal transform based SPIs' advantages are as follows: First, it can reconstruct the object image without distortion. Second, it can also make better use of the sparsity of natural images in the transform domain to reconstruct high-quality object images by only obtaining larger coefficients in the transform domain, while the compressed sensing method reconstructs object images by dealing with coefficients corresponding to the random patterns without distinction. Third, it is only a simple two-dimensional inverse transformation, so the operation time can be ignored. By contrast, a compressed sensing algorithm takes more time to reconstruct the image.

Besides，our method has the following advantages：First，a threshold can be adaptively set according to the expected imaging fidelity. The method can achieve a balance between imaging speed and the expected imaging fidelity. Second，it can adaptively reduce the sampling rate，thus it can adaptively improve the imaging speed of the SPI significantly. Third，we can further investigate the influence of the dark noise of the PD on SPI. Experimental results show that the proposed adaptive zigzag sampling is capable of automatically reducing the influence of the high-frequency dark noise on the reconstruction quality by setting an appropriate threshold C to get better reconstructions.

4 Conclusion

We proposed and demonstrated the Hadamard SPI using the proposed adaptive oblique zigzag sampling method. Experimental results show that it can adaptively reduce the sampling rate while meeting the fidelity required by users by setting a threshold. In other words，it can adaptively achieve a balance between imaging quality and speed. When the dark noise of the PD is high，the advantage of the proposed method is highlighted. Since when the dark noise of the imaging system is high and the high-frequencies of the object to be reconstructed are drowned in the noise，SPI using the fully sequential or zigzag sampling will not give a satisfactory result. However，SPI using the proposed method can automatically discard the high-frequency noise by setting an appropriate threshold C to get a better reconstruction，at the same time a balance between imaging quality and speed can be achieved.

References

[1] DONOHO D L. Compressed sensing[J]. IEEE Transactions on Information Theory，2006，52(4):1289-1306.

[2] CANDÈS E J，ROMBERG J，TAO T. Robust uncertainty principles ：exact signal frequency information[J]. IEEE Transactions on Information Theory，2006，52(2):489-509.

[3] DUARTE M F，DAVENPORT M A，TAKHAR D，et al. Single-pixel imaging via compressive sampling[J]. IEEE Signal Processing Magazine，2008，25(2):83-91.

[4] CHAN W L，CHARAN K，TAKHAR D，et al. A single-pixel terahertz imaging system based on compressed sensing[J]. Applied Physics Letters，2008，93(12):S293.

[5] RYOICHI H，HIROAKI M，JUN T . Single-pixel compressive diffractive imaging[J]. Applied Optics，2017，56(14): 4085-4089.

[6] JIANG Shan，LI Xianye，ZHANG Zexin，et al. Scan efficiency of structured illumination in iterative single pixel imaging [J]. Optics Express，2019，27(16):22499.

[7] MA Haiyu，SANG Aijun，ZHOU Cheng，et al. A zigzag scanning ordering of four-dimensional Walsh basis for single-pixel imaging[J]. Optics Communications ，2019，443：69-75.

[8] PRATT W K，KANE J，ANDREWS H C . Hadamard transform image coding[J]. Proceedings of the IEEE，1969，57 (1):58-68.

[9] DECKER J J A. Hadamard-transform image scanning[J]. Applied Optics，1970，9(6):1392-1395.

[10] EDGAR M P，GIBSON G M，BOWMAN R W，et al. Simultaneous real-time visible and infrared video with single-pixel detectors[J]. Scientific Reports. 2015，5(1):745-755.

[11] SUN Mingjie，EDGAR M P，PHILLIPS D B，et al. Improving the signal-to-noise ratio of single-pixel imaging using digital microscanning[J]. Optics Express，2016，24(10):10476-10485.

[12] ZHANG Zibang，JIAO Shuming，YAO Manhong，et al. Secured single-pixel broadcast imaging[J]. Optics Express，2018，26(11):14578.

[13] LOCHOCKI B，GAMBÍN A，MANZANERA S，et al. Single pixel camera ophthalmoscope[J]. Optica，2016，3(10): 1056-1059.

[14] ZHANG Zibang，WANG Xueying，ZHENG Guoan，et al. Hadamard single-pixel imaging versus Fourier single-pixel imaging[J]. Optics Express，2017，25(16):19619-19639.

[15] GIBSON G，JOHNSON S，PADGETT M . Single-pixel imaging 12 years on：a review [J]. Optics Express，2020，28 (19)：28190－28207.

[16] ZHANG Zibang，LIU Shijie，PENG Junzheng.Simultaneous spatial，spectral，and 3D compressive imaging via efficient Fourier single-pixel measurements[J]. Optica ，2018，5：315-319.

[17] ZHANG Zibang，MA Xiao，ZHONG Jingang. Single-pixel imaging by means of Fourier spectrum acquisition[J]. Nature Communications，2014，6:6225.

[18] ZHANG Zibang，ZHONG Jingang. Three-dimensional single-pixel imaging with far fewer measurements than effective image pixels[J]. Optics Letters，2016，41(11):2497.

［19］ JIANG Hongzhi，ZHU Shuguang，ZHAO Huijie，et al. Adaptive regional single-pixel imaging based on the Fourier slice theorem.［J］. Optics Express，2017，25(13):15118-15130.

［20］ ZHANG Zibang，WANG Xueying，ZHENG Guoan，et al. Fast Fourier single-pixel imaging via binary illumination［J］. Scientific Reports，2017，7(1):12029.

［21］ ZHANG Zibang，LU Tianao，PENG Junzheng，et al. Fourier single-pixel imaging techniques and applications［J］. Infrared and Laser Engineering，2019，48(6)：0603002

［22］ ALEMOHAMMAD M，STROUD J R，BOSWORTH B T，et al. High-speed all-optical Haar wavelet transform for real-time image compression［J］. Optics Express，2017，25(9):9802.

［23］ XU Zihao，CHEN Wen，JOSÉ P，et al. 1000 fps computational ghost imaging using LED-based structured illumination ［J］. Optics Express，2018，26(3):2427-2434.